THE EUROPEAN SOCIETY OF MEDICINE
Medical Research Archives, Volume 12 Issue 7

RESEARCH ARTICLE

Objective evaluation of liver fibrosis using ultrasound microscopy

Katsutoshi Miura[1], Toshihide Iwashita[1]

[1]Department of Regenerative & Infectious Pathology, Hamamatsu University School of Medicine

OPEN ACCESS

PUBLISHED
31 July 2024

CITATION
Miura, K and Iwashita T., 2024. Objective evaluation of liver fibrosis using ultrasound microscopy. Medical Research Archives, [online] 12(7). https://doi.org/10.18103/mra.v12i7.5611

DOI
https://doi.org/10.18103/mra.v12i7.5611

ISSN
2375-1924

ABSTRACT

Background: Chronic liver damage, such as viral hepatitis, causes liver fibrosis. Recently, the advent of interferon (INF) and antiviral drugs has reduced hepatitis viruses, enabling liver function recovery and fibrosis improvement. A quantitative assessment of liver fibrosis is mandatory to identify treatment efficacy.

Aim: We aimed to apply speed-of-sound (SOS) values for the objective assessment of fibrosis in liver biopsy because SOS values correlate with stiffness.

Methods: We differentiated SOS images of pre- and post-treatment INF liver. We then compared the SOS values with the fibrosis score and magnetic resonance elastography (MRE) values. We tried to digest sections with collagenase to clarify the process of fibrosis deletion.

Results: After INF therapy, SOS images demonstrated a marked reduction in fibrosis in the lobules. SOS values were well correlated with the fibrosis score and slightly corresponded to MRE values. Perisinusoidal fibrosis was susceptible to collagenase digestion. Portal areas were minimal.

Conclusion: The SOS value, which objectively evaluates fibrosis in tissue sections, is an excellent indicator. It assesses fibrosis progression and reduction post-treatment.

Introduction

Chronic liver damage eventually causes cirrhosis. Viral infection, such as hepatitis C viruses (HCV), is a leading cause of liver cirrhosis.[1] Recently, the advent of interferon (INF) and antiviral drugs has reduced or eliminated hepatitis viruses, enabling liver function recovery and fibrosis improvement.[2–5] Methods to assess liver fibrosis include blood biochemistry, such as platelet count, prothrombin time, albumin, total bilirubin, and serum aminotransferase levels,[6] magnetic resonance imaging,[7] and ultrasound.[8] However, liver biopsy as the gold standard has been utilized for grading inflammatory activity and staging the amount of fibrosis,[9,10] both predictors of patient prognosis and outcome.[11]

Liver fibrosis is identified as F0–F4 (cirrhosis) based on histopathological images, but this is a subjective judgment that warrants special stains, such as Sirius Red,[12] Masson Trichrome,[13] and Elastica van Gieson.[14]

Here, we present a method for the objective assessment of fibrosis in liver biopsy tissue using ultrasound microscopy. This method is based on the correlation between speed-of-sound (SOS) with tissue stiffness and uses the liver lobule SOS as a proxy for fibrosis severity.[15–17]

SOS values through each point on the section are plotted on the screen to make histological images using the same flat section[15,16].

The relationship between the SOS and elastic bulk modulus of a liquid-like medium can be represented using the Newton–Laplace equation as follows[18]:

$$c = (K / \rho)^{1/2}$$

where c is the SOS, K is the bulk modulus of elasticity, and ρ is the density.

Thus, the SOS increases with material stiffness (the resistance of an elastic body to deformation by an applied force) but decreases with density. As the thin sections were soaked in water during the measurement period, the average soft tissue density was nearly 1 g/cm, and the SOS through the soft tissues was strongly correlated with their stiffness[19].

In this study to reveal the utility of SOS images, we first compared fibrosis before and after INF treatment for HCV. We selected two cases that showed sustained virologic response (SVR) after INF therapy. Then, we compared SOS values with magnetic resonance elastography (MRE) and histological fibrosis scores to evaluate accuracy of SOS values. Moreover, liver susceptibility to collagenase digestion was assessed over time to estimate the histological process of collagen disappearance using SOS values.

Materials and methods

SAMPLE PREPARATION

This study used stored specimens for pathological diagnosis. Verbal and written informed consent were obtained from each patient before sample collection. This study did not use names and other identifying information. The study protocol conformed to the ethical guidelines of the Declaration of Helsinki and was approved by the ethics committee of Hamamatsu University School of Medicine (approval no. 19-180). All participants signed written informed consent. All procedures were conducted following the guidelines and regulations of the ethics committee. Tissue samples for pathological diagnosis were fixed in 10% buffered formalin, embedded in paraffin, and cut into flat slices (10-μm-thick sections were made for SAM, whereas 4-μm-thick sections were prepared for light microscopy).

SAM OBSERVATIONS

A SAM system (AMS-50AI; Honda Electronics, Toyohashi Aichi, Japan) with a central frequency of 320 MHz and lateral resolution of 3.8-μm,[20,21,22] was used to evaluate liver specimens, as previously reported. The transducer was excited by a 2-ns electrical pulse to emit an acoustic pulse.[23] Samples were placed on the transducer, and distilled water was used as the coupling fluid between the transducer

and specimen. The transducer was utilized for both signal transmission and reception. Waveforms, reflected from the surface and bottom of the sample, were compared to measure each point's SOS and thickness. The waveform that was obtained from a glass surface served as the reference value of SOS at 1485 m/s through water.

The specimens were evaluated using a previously reported method,[24] without modifications. Briefly, the mechanical scanner was arranged such that the ultrasonic beam was over the specimen to provide the SOS value at each point. The distance between the transducer and the specimen was adjusted to correctly identify the pulse wave. The scan width and line were 2.4, 1.2, 0.6, and 0.3 mm^2. The sampling points were 300 in one scanning line and width, and each square frame included 300 × 300 points. Data from four scans were averaged to identify the value of each scan point to reduce noise interference. The mean SOS value of each component was calculated from five separate areas. The values in the region of interest on the screen were recorded to determine the SOS values.

LM OBSERVATION OF INFLAMMATION AND FIBROSIS

The same or nearby SAM sections were stained with hematoxylin and eosin, Elastica van Gieson, or Elastica–Masson's trichrome for comparison.

Liver tissues were assessed for inflammatory activity and fibrosis following the new Inuyama classification.[9] The degrees of hepatic inflammation and fibrosis were scored according to the classification from A0–A3 and from F0–F4, respectively.

COLLAGENASE DIGESTION

Dewaxed paraffin sections were soaked in distilled water and submerged in a phosphate-buffered saline solution containing 0.5-mM calcium chloride (pH of 7.4) and 250 units/mL of type 3 collagenase (Worthington, Lakewood, NJ, USA) at 37 ℃ for 1, 3, and 6 h. The collagenase used in the present study was selected for its substrate specificity to collagen, which has lower proteolytic activity than other collagenases. Digested sections were washed with distilled water before SAM observation. The same sections were measured at 1, 3, and 6 h after digestion.

SOS COMPARISON OF PRE- AND POST-TREATMENT FIBROSIS IN INF-TREATED PATIENTS WITH HCV

Two patients who demonstrated a sustained virological response (SVR) to HCV with IFN treatment were compared with liver histology pre- and post-treatment. They underwent partial hepatectomy due to hepatocellular carcinoma occurring after SVR. This study used liver sections from distant carcinoma portions. The SOS images and corresponding LM images were compared pre- and post-treatment.

COMPARISON OF FIBROSIS EVALUATION BY OPTICAL MICROSCOPY, MRE, AND SOS

Six different cases were compared according to fibrosis scores, MRE values, and SOS values of the lobules. MRE was performed to quantify liver stiffness using a fibroscan instrument.

CHANGES IN SOS VALUES OVER TIME AFTER COLLAGENASE DIGESTION

We tried to digest sections with collagenase to clarify the process of fibrosis deletion. SOS and LM images were used for histological analysis of liver specimens with different fibrosis stages soaked in collagenase.

STATISTICAL ANALYSES

The mean SOS values were calculated from at least five areas per structure. One-way analysis of variance (ANOVA) with Tukey–Kramer post-hoc tests were conducted to evaluate the SOS difference between pre- and post-treatment and the reduction rate of post-collagenase digestion and, among SOS values, fibrosis score, and MRE values. Multiple comparisons using the Tukey–Kramer test were utilized to assess the significance of changes within each independent variable.

Pearson's correlation coefficient test was utilized to compare SOS, fibrosis score, and MRE values. Software for SAM (LabView 2012, National Instruments, Austin, TX, USA) and commercial statistics software (BellCurve for Excel; Social Survey Research Information, Tokyo, Japan) were used to calculate areas-of-interest values and analyze ANOVA and Tukey–Kramer post-hoc test results. All datasets were assessed for normal distribution and homogeneity of variance using the Bartlett or Levine test before performing the Tukey–Kramer test. An ANOVA table was prepared to investigate the presence of different mean values among groups if the variances were equal. The Tukey–Kramer test was used to determine groups with significantly different mean values in the presence of different means. A generalization of the two-sample Welch or Brown–Forsythe test was used in the case of non-equal variances. A *p*-value of <0.05 was considered statistically significant for all analyses.

Results

SOS COMPARISON OF PRE- AND POST-TREATMENT FIBROSIS IN INF-TREATED PATIENTS WITH HCV

SOS images of the livers of patients who had improved to SVR after IFN treatment were compared (Figs. 1A and 1B). Table 1 shows laboratory data before and after INF treatment. SOS images demonstrate marked fibrosis reduction in the lobules. Fibrous portal expansion remained in case 1 but disappeared in case 2. Additionally, the fibrosis in the portal area was reduced, although mildly.

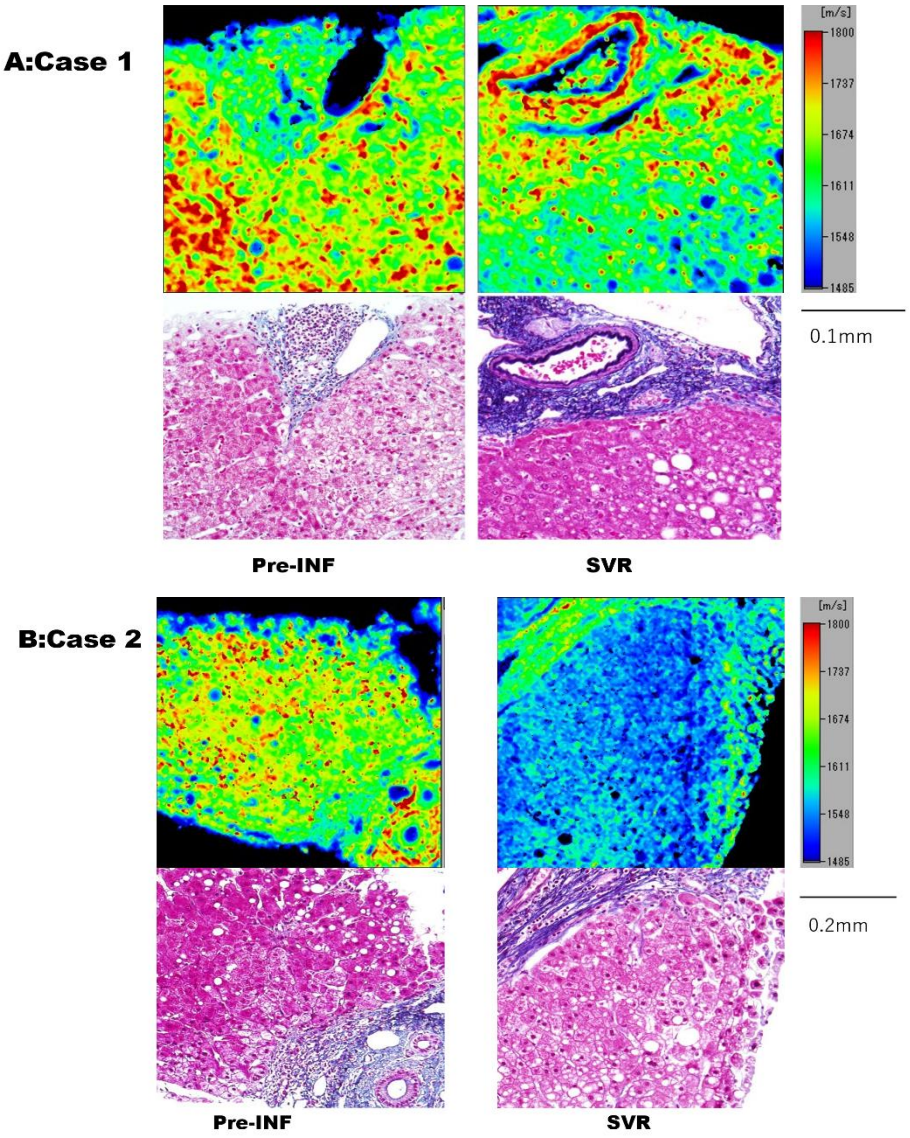

Figure 1. SOS images and Masson's trichrome staining before and after INF treatment (A: case 1, B: case 2)

In case 1, the liver stage was at F2A2 before INF therapy, and the liver recovered to F1A1 while maintaining SVR. Additionally, case 2 changed the liver stage from F2A2 to F1A1, 8 years after INF therapy. SOS images before IFN treatment demonstrated reticular lobules with high SOS areas along the sinusoid, which corresponded to perisinusoidal fibrosis in the LM images. The high SOS areas remained post-treatment in the periportal area in case 1 and almost disappeared in case 2.

Masson's trichrome staining shows portal lymphocytic infiltration and irregular arrays of hepatocytes in the lobule pre-treatment, which improved post-treatment. Perisinusoidal fibrosis is not evident in this condition.

Table 1. Laboratory results of the two patients with hepatitis C before and after IFN treatment

	Case 1 before	after (4 year)	**Case 2** before	after (8 year)
AST(IU/L)	59	44	52	15
ALT(IU/L)	35	44	171	17
Platelets(x 10^4/ml)	17.9	19.5	19	24.2
Total bilirubin (mg/dl)	0.7	1	0.7	0.4
Albumin (g/dl)	3.4	4.3	3.6	4.2
PT activity (%)	86	96		111
γ−GTP	175	261	175	
HCV-RNA		ND		ND

AST: aspartate aminotransferase; ALT: alanine aminotransferase; γ-GTP: gamma-glutamyl transpeptidase; ND: not detected.

LM images via Elastica–Masson's trichrome staining demonstrated irregular hepatocyte arrangement with perisinusoidal fibrosis observed pre-INF, which improved after SVR.

The mean SOS values (± standard deviation) of the pre-INF lobules were 1632.2 ± 48.2 m/s and 1639.5 ± 49.8 m/s in cases 1 and 2, respectively (Fig. 2). The SOS values post-treatment decreased to 1614.5 ± 38.2 and 1564.4 ± 26.7 m/s, respectively. The statistical comparison of mean SOS values exhibited a significant decline in both cases ($P < 0.01$).

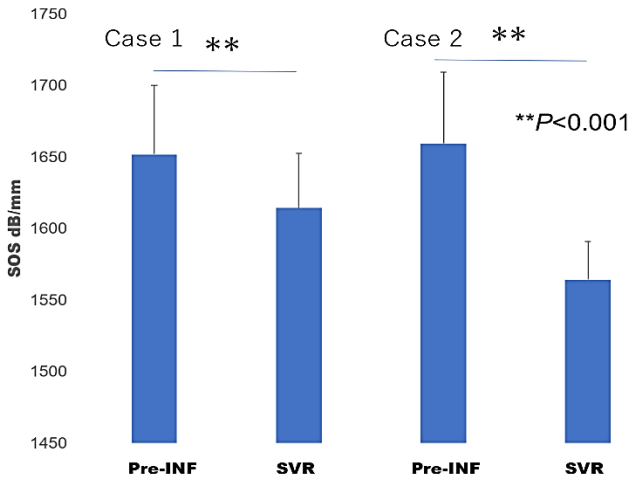

Figure 2. Comparison of the average SOS of the lobules before and after INF therapy
SOS values significantly decreased post-treatment ($P < 0.01$). SVR: sustained virological response

COMPARISON OF THE EVALUATION OF FIBROSIS BY OPTICAL MICROSCOPY, MRE VALUES, AND SOS IMAGES

Fig. 3 compares SOS images with LM images of different fibrosis scores and MRE values. Periportal fibrosis became sharper on SOS images than on LM images and increased with fibrous scores and MRE values.

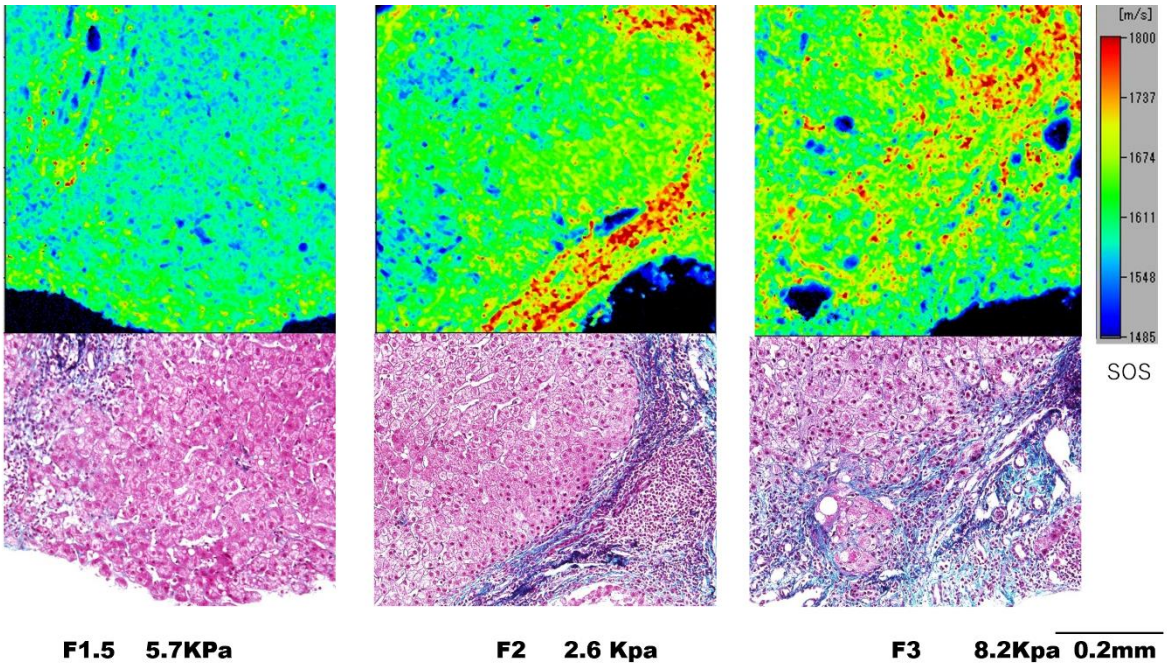

Figure 3. Comparison of SOS and LM images at different liver fibrosis stages
SOS images (upper row) and Elastica–Masson's trichrome staining (lower row) showing livers of F1, F2, and F3 with MRE values. The SOS values of lobules increase with severe portal fibrosis.

Table 2 shows the clinical data of liver stages, mean lobular SOS values, and MRE values of six different cases. Fig. 4 illustrates the correlation among SOS values, fibrosis scores, and MRE values of lobules. Six cases were arranged in order of low fibrosis score. The correlation coefficients were 0.975 and 0.605 between SOS and fibrosis score, and SOS and MRE, respectively. SOS values were strongly positively correlated with fibrosis score ($p < 0.001$). SOS was positively correlated with MRE values, but the correlation was not as strong as the fibrosis score ($p < 0.20$).

Table 2. Laboratory data of six patients with hepatitis C at SVR

Case No	1	2	3	4	5	6
Age Sex	54F	76F	75F	72M	54M	67M
AST(IU/L)	23	22	27	27	66	50
ALT(IU/L)	16	13	20	16	81	52
Platelets(x 10^4/mL)	19.7	11.7	15.7	14.3	14.7	15.9
Total bilirubin (mg/dL)	0.7	1	0.6	0.9	0.8	0.7
Albumin (g/dL)	4.5	4.5	4	4.8	4.2	4
γ—GTP (IU/L)	18	19	16	21	23	52
AFP (ng/mL)	4	0.5	5	3	3	5
HCV-RNA	ND	ND	ND	ND	ND	ND
Fibrosis score	F0	F1.5	F2	F2	F2.5	F3
SOS of lobule m/s	1557.3	1595.4	1630.3	1621.4	1656.4	1659.1
MRE Kpa	1.9	5.7	2.6	3.7	4.8	8.2

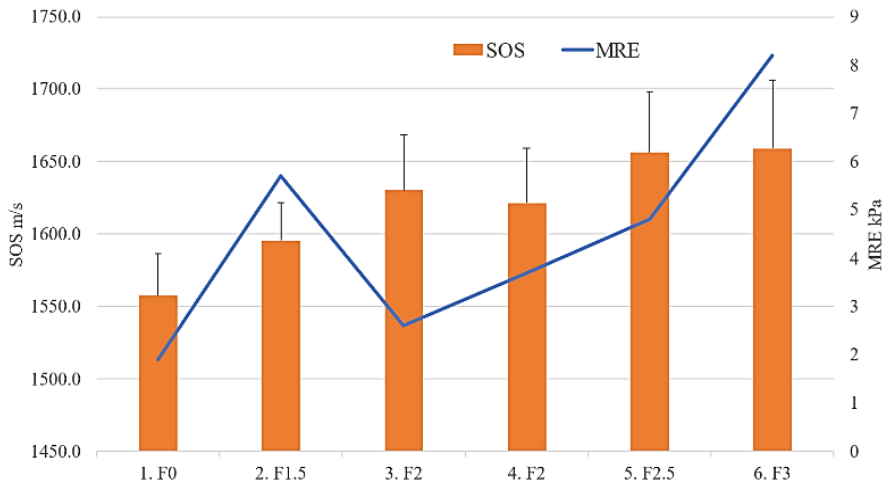

Figure 4. Comparison of the mean lobule SOS (± standard deviation) and MRE
Six cases were arranged in order of low fibrosis score. SOS and MRE values increased with fibrosis scores. The correlation coefficients were 0.975 and 0.605 between SOS and fibrosis score, and SOS and MRE, respectively. SOS values and fibrosis scores demonstrated a strong positive correlation ($p < 0.001$). SOS and MRE values exhibited not so great correlation ($p < 0.20$).

CHANGES IN SOS VALUES OVER TIME AFTER COLLAGENASE DIGESTION

SOS values in the hepatic lobules decreased predominantly over time after collagenase digestion (Figs. 5A, 5B), with a conspicuous decrease in SOS values in the fibrosis of the perisinusoidal region in the lobules (Fig. 6). The decrease in SOS in the portal area of Gleason sheath was smaller than that in the lobules.

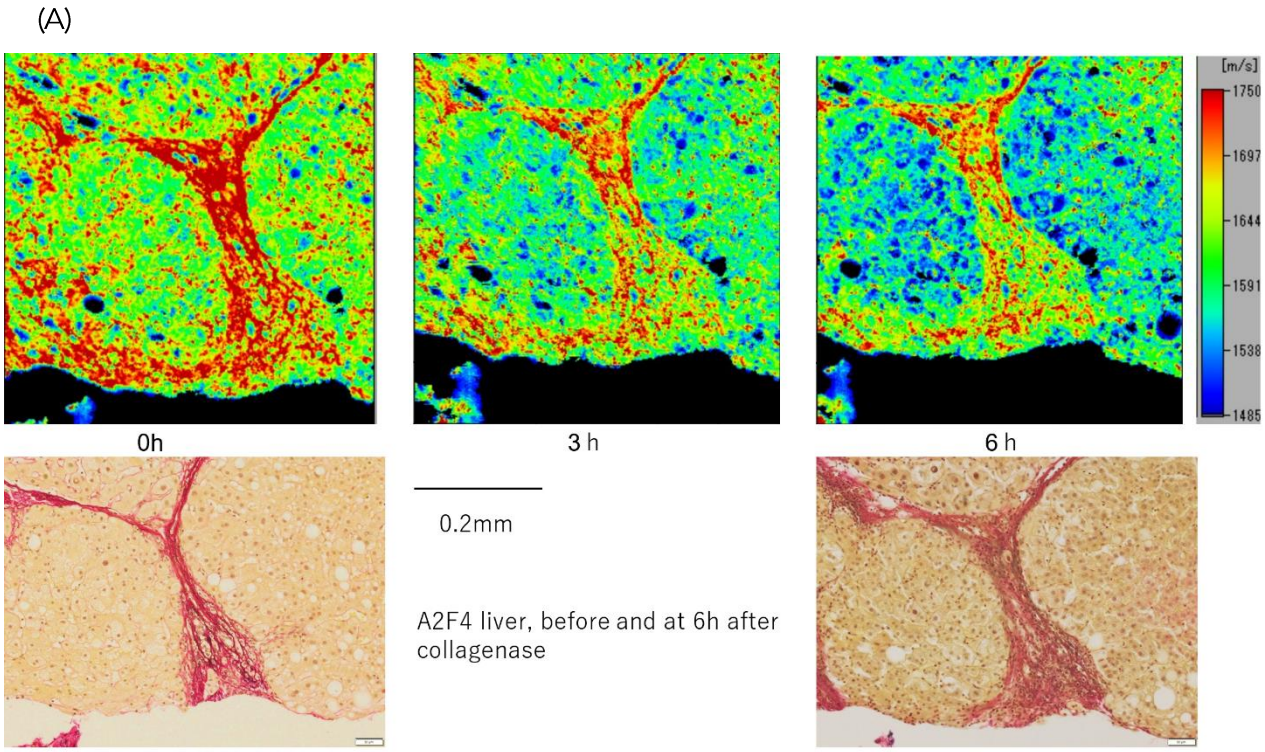

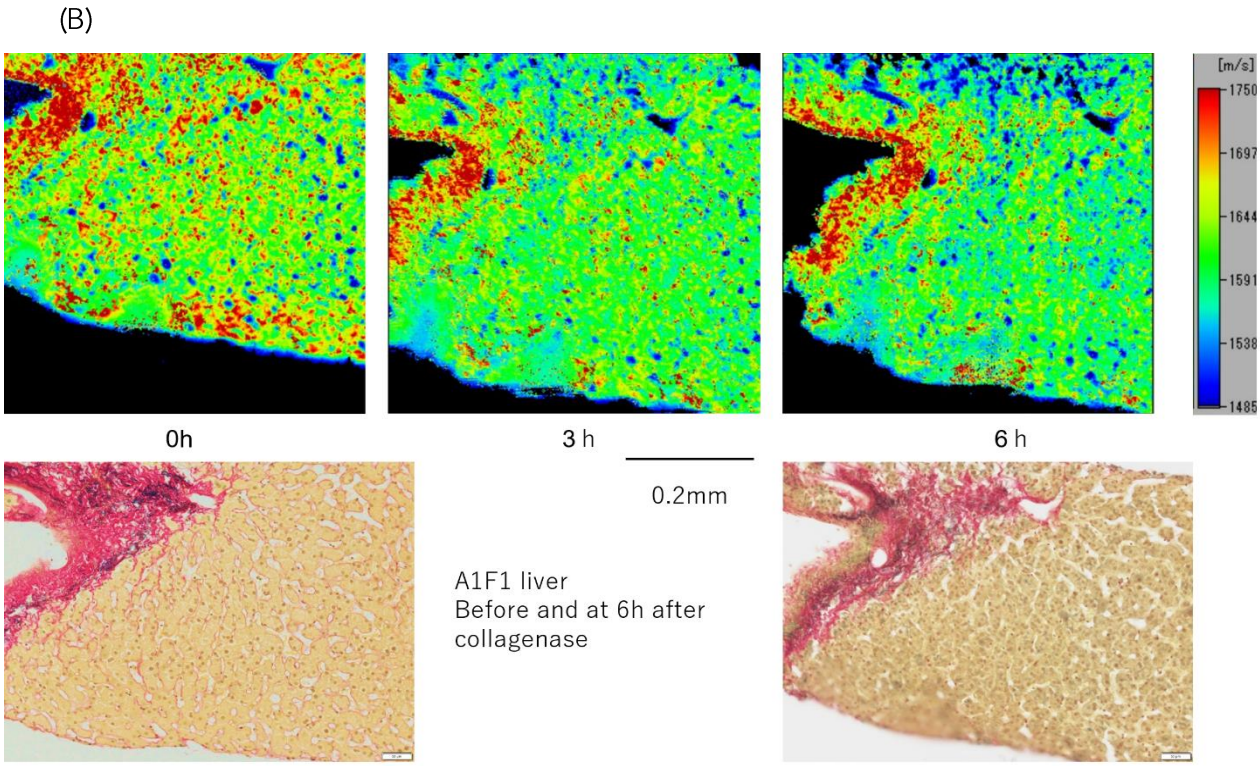

Figure 5. SOS and LM images after collagenase digestion
A2F4 (A) and A1F1 (B) livers were digested using collagenase, followed by SOS images after digestion. High SOS values in the lobular and portal areas gradually decrease after collagenase digestion, corresponding to perisinusoidal and portal fibrosis observed in Elastica van Gieson staining.

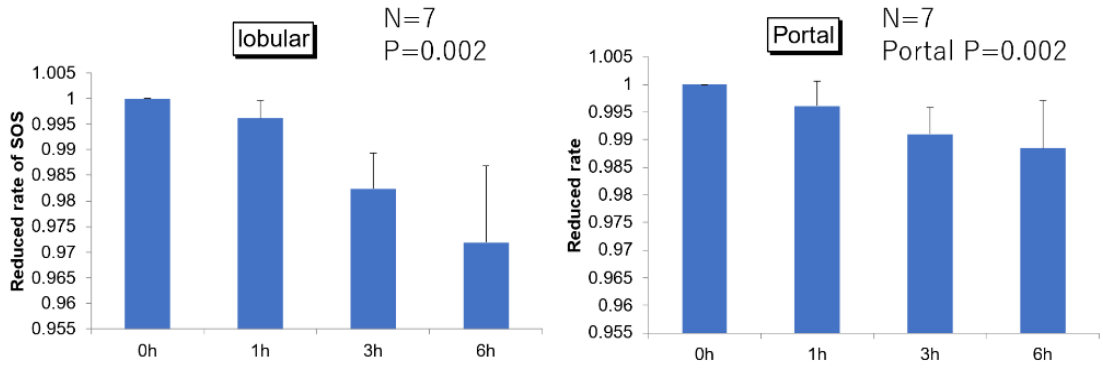

Figure 6. Alteration in the reduction rates of mean SOS in the lobular and portal areas after collagenase digestion
Both lobular and portal rates were significantly reduced (both $P = 0.002$) after digestion. The lobular reduction was more conspicuous than portal reduction, which involved thicker collagen bundles.

Discussion

Ultrasound has been widely used for detecting liver diseases both in vivo and in vitro. In clinical practice, abdominal echo and elastography serve as non-invasive, rapid, and painless methods. To scan deep liver tissue from the abdominal surface, a wave frequency between 3 to 10 MHz is employed. Although higher frequency enhances spatial resolution, in vivo observation prioritizes reach over resolution.

For detecting cellular alterations related to liver diseases, a frequency of at least 80 MHz is necessary to identify cells. Researchers have utilized ultrasound to measure parameters such as SOS, attenuation, and backscatter coefficient across a wide range of methods[25]. Notably, SOS has proven superior to attenuation or backscattering characteristics for distinguishing between tumor and normal liver tissues[26].

In a study by Irie et al., SOS was employed to investigate liver fibrosis using 80 and 250 MHz transducers[27] The 250-MHz transducer demonstrated better spatial resolution for studying fibrosis and hepatocytes.

Recently, we encountered two cases of hepatocellular carcinoma arising from SVR patients with HCV after INF treatment. While functional recovery from liver fibrosis was evident, objective histological evaluation posed challenges due to local variation. We attempted to use SOS values to assess liver fibrosis in this study.

SOS imaging provides an effective method for visualizing liver fibrosis in tissue sections. Unlike LM images, SOS images are inherently digital and yield objective, comparable values. Assessment using unstained 10-μm thick sections appeared suitable for accurate fibrosis evaluation, minimizing bias from staining variation and providing rich collagen information. SOS values correlated with fibrosis scores, enabling accurate assessment of progression or improvement post-treatment, as depicted in Figures 3 and 4. However, a drawback of biopsy-based assessment is that local fibrosis may not fully represent overall liver fibrosis, which explains why SOS values did not correlate with MRE values.

Collagenase digestion is more sensitive in the periportal area than in the portal. Periportal collagen fibers are thin along the sinusoid, while portal collagen fibers are thick. The portal areas originally contain abundant collagen. Old collagen, due to glycation and intermolecular cross-linking[28], resists protein degradation. Our research has detected old collagens based on SOS values, which are challenging to break down using collagenase.[24,29–31]

The SOS value serves as an excellent fibrosis indicator, evaluating fibrosis progression and reduction post-treatment. However, this study has limitations. First, the sample size required to assess the association among SOS values, MRE values, and function was limited. Rebiopsy is usually unnecessary after liver function remission. Second, formalin-fixed paraffin-embedded sections were used in this study. Fixation effects (duration and temperature) may introduce bias in SOS values. Pre-IFN biopsy samples underwent 1–3 days of fixation at room temperature. Surgical samples had longer fixation duration than biopsy samples, potentially inducing hyper-fixation to increase tissue SOS values. However, post-treatment operation samples showed decreased SOS values (Fig. 1), with minimal variation due to fixation conditions. Third, extrinsic collagenase from bacteria digests liver collagens within 3–8 hours. In vivo, collagenase-producing cells (e.g., macrophages) take much longer to break down collagen, playing a crucial role in collagen reduction.[32]

Understanding the association between hepatic stellate cells or Ito cells (which store vitamin A in a healthy state) and fibrosis is an area of interest.[33]

The reduction of perisinusoidal fibrosis was evident in HCV-related fibrosis. However, this result may not apply to other fibrosis types with different causes. Evaluating recovery through fibrosis treatment applies not only to HCV but also to alcoholic, nonalcoholic steatohepatitis, congestive, and drug-related hepatitis. Collecting more cases is crucial for further investigation.

Conclusion

SOS imaging effectively visualizes liver fibrosis, comparable to fibrosis progression or regression based on SOS values. SOS images exhibit high resolution and positively correlate with LM images. Collagenase digestion predicts recovery susceptibility from fibrosis.

Conflicts of Interest Statement:

KM received supporting fees for attending meetings from Honda Electronics. TI has no conflicts of interest to declare.

Acknowledgments:

The authors acknowledged Dr. Yoshimasa Kobayashi of the Department of Medicine, Hamamatsu University School of Medicine for the clinical data presentation of the patients, and Drs. Yuki Egawa and Toshiaki Moriki at Shizuoka City Hospital, and Mr. Yuki Kurita and Yuta Inaba at Advanced Research Facilities & Services, Hamamatsu University School of Medicine for the sample preparation. Drs. Kanna Yamashita, Michio Fujie, and Toshi Nagata of the Department of Health Science, Hamamatsu University School of Medicine provided the research facilities for this study.

References:

1. Freeman AJ, Dore GJ, Law MG, et al. Estimating progression to cirrhosis in chronic hepatitis C virus infection. *Hepatology*. 2001;34(4 I):809-816. doi:10.1053/jhep.2001.27831

2. Saldarriaga OA, Dye B, Pham J, et al. Comparison of liver biopsies before and after direct-acting antiviral therapy for hepatitis C and correlation with clinical outcome. *Sci Rep*. 2021;11(1). doi:10.1038/s41598-021-93881-7

3. Chu CY, Cheng CH, Chen HL, et al. Long-term histological change in chronic hepatitis C patients who had received peginterferon plus ribavirin therapy with sustained virological response. *Journal of the Formosan Medical Association*. 2019;118(7):1129-1137. doi:10.1016/j.jfma.2018.11.005

4. Hsieh MH, Kao TY, Hsieh TH, et al. Long-term surveillance of liver histological changes in chronic hepatitis C patients completing pegylated interferon-α plus ribavirin therapy: an observational cohort study. *Ther Adv Chronic Dis*. 2022;13. doi:10.1177/20406223211067631

5. Shiffman ML, Sterling RK, Contos M, et al. *Long Term Changes in Liver Histology Following Treatment of Chronic Hepatitis C Virus*. Vol 13.; 2014.

6. Chen Z, Ma Y, Cai J, et al. Serum biomarkers for liver fibrosis. *Clinica Chimica Acta*. 2022;537. doi:10.1016/j.cca.2022.09.022

7. Faria SC, Ganesan K, Mwangi I, et al. MR imaging of liver fibrosis: Current state of the art. *Radiographics*. 2009;29(6):1615-1635. doi:10.1148/rg.296095512

8. Lin YS. Ultrasound Evaluation of Liver Fibrosis. *J Med Ultrasound*. 2017;25(3):127-129. doi:10.1016/j.jmu.2017.04.001

9. Ichida F, Tsuji T, Omata M, et al. New Inuyama classification; new criteria for histological assessment of chronic hepatitis. International

Hepatology Communications. *Itemational Hepatology Communications*. 1996;6:112-119.

10. Goodman ZD. Grading and staging systems for inflammation and fibrosis in chronic liver diseases. *J Hepatol*. 2007;47(4):598-607. doi:10.1016/j.jhep.2007.07.006

11. Heyens LJM, Busschots D, Koek GH, Robaeys G, Francque S. Liver Fibrosis in Non-alcoholic Fatty Liver Disease: From Liver Biopsy to Non-invasive Biomarkers in Diagnosis and Treatment. *Front Med (Lausanne)*. 2021;8. doi:10.3389/fmed.2021.615978

12. Astbury S, Grove JI, Dorward DA, Guha IN, Fallowfield JA, Kendall TJ. Reliable computational quantification of liver fibrosis is compromised by inherent staining variation. *Journal of Pathology: Clinical Research*. 2021;7(5):471-481. doi:10.1002/cjp2.227

13. Lo RC, Kim H. Histopathological evaluation of liver fibrosis and cirrhosis regression. *Clin Mol Hepatol*. 2017;23(4):302-307. doi:10.3350/cmh.2017.0078

14. Abe T, Hashiguchi A, Yamazaki K, et al. Quantification of collagen and elastic fibers using whole-slide images of liver biopsy specimens. *Pathol Int*. 2013;63(6):305-310. doi:10.1111/pin.12064

15. Saijo Y. Recent Applications of Acoustic Microscopy for Quantitative Measurement of Acoustic Properties of Soft Tissues. In: Mamou J, Oelze M, eds. *Quantitative Ultrasound in Soft Tissues*. Springer; 2013:291–313. doi:10.1007/978-94-007-6952-6_12

16. Miura K. Application of Scanning Acoustic Microscopy to Pathological Diagnosis. In: Stanciu SG, ed. *Microscopy and Analysis*. Intech; 2016: 381-403. doi:10.5772/63405

17. Saijo Y, Filho E, Sasaki H, et al. Ultrasonic Tissue Characterization of Atherosclerosis by a Speed-of-Sound Microscanning System. *IEEE Trans Ultrason Ferroelectr Freq Control*. 2007;54(8):1571 -1577.

18. Saijo Y. Acoustic microscopy: latest developments and applications. *Imaging Med*. 2009; 1(1):47-63. doi:http://dx.doi.org/10.2217/iim.09.8

19. Azhari H. Appendix A: Typical Acoustic Properties of Tissues. *Basics of Biomedical Ultrasound for Engineers*. Published online 2010: 313-314. doi:10.1002/9780470561478.app1

20. Miura K, Mineta H. Histological evaluation of thyroid lesions using a scanning acoustic microscope. *Pathol Lab Med Int*. 2014;6:1-9.

21. Miura K, Yamamoto S. Histological imaging from speed-of-sound through tissues by scanning acoustic microscopy (SAM). *Protoc Exch*. Published online 2013. doi:10.1038/protex.2013.040

22. Tamura K, Ito K, Yoshida S, Mamou J, Miura K, Yamamoto S. Alteration of speed-of-sound by fixatives and tissue processing methods in scanning acoustic microscopy. *Front Phys*. 2023;11. doi:10.3389/fphy.2023.1060296

23. Hozumi N, Yamashita R, Lee CK, et al. Time-frequency analysis for pulse driven ultrasonic microscopy for biological tissue characterization. In: *Ultrasonics*. Vol 42. ; 2004:717-722. doi:10.1016/j.ultras.2003.11.005

24. Miura K, Yamashita K. Mechanical weakness of thoracic aorta related to aging or dissection predicted by speed of sound with collagenase. *Ultrasound Med Biol*. 2019;45(12):3102-3115. doi:10.1016/j.ultrasmedbio.2019.08.012

25. Meziri M, Pereira WCA, Abdelwahab A, Degott C, Laugier P. In vitro chronic hepatic disease characterization with a multiparametric ultrasonic approach. *Ultrasonics*. 2005;43(5):305-313. doi:10.1016/j.ultras.2004.09.002

26. Bamber JC, Hill CR. Acoustic properties of normal and cancerous human liver-1. Dependence on pathological condition. *Ultrasound in Med & Biol*. 1981;7:121-133.

27. Irie S, Inoue K, Yoshida K, et al. Speed of sound in diseased liver observed by scanning

acoustic microscopy with 80 MHz and 250 MHz. *J Acoust Soc Am*. 2016;139(1):512-519. doi:10.1121/1.4940126

28. Uceda AB, Mariño L, Casasnovas R, Adrover M. An overview on glycation: molecular mechanisms, impact on proteins, pathogenesis, and inhibition. *Biophys Rev*. 2024;16(2):189-218. doi:10.1007/s12551-024-01188-4

29. Miura K, Katoh H. Structural and histochemical alterations in the aortic valves of elderly patients: a comparative study of aortic stenosis, aortic regurgitation, and normal valves. *Biomed Res Int*. Published online 2016. doi:10.1155/2016/6125204

30. Miura K, Yamashita K. Evaluation of aging, diabetes mellitus, and skin wounds by scanning acoustic microscopy with protease digestion. *Pathobiology of Aging & Age-related Diseases*. Published online 2018. doi:10.1080/20010001.2018.1516072

31. Miura K. Histological and mechanical information based on biochemical alterations of cardiovascular diseases using scanning acoustic microscopy with P proteinases : A novel technique for cardiovascular research. *Atherosclerosis: Open Access*. 2021;6(2).

32. Cheng D, Chai J, Wang H, Fu L, Peng S, Ni X. Hepatic macrophages: Key players in the development and progression of liver fibrosis. *Liver International*. 2021;41(10):2279-2294. doi:10.1111/liv.14940

33. Sufleţel RT, Melincovici CS, Gheban BA, Toader Z, Mihu CM. Hepatic stellate cells - from past till present: Morphology, human markers, human cell lines, behavior in normal and liver pathology. *Romanian Journal of Morphology and Embryology*. 2020;61(3):615-642. doi:10.47162/RJME.61.3.01